JOURNAL OF THERMOPHYSICS AND HEAT TRANSFER
Vol. 15, No. 4, October–December 2001

Shock Propagation Through a Low-Pressure Glow Discharge in Argon

A. R. White* and V. V. Subramaniam†
The Ohio State University, Columbus, Ohio 43210

Experimental measurements recording spark-generated shock propagation characteristics within an argon glow discharge and in the afterglow region are reported here. Photoacoustic deflection is used to measure average shock speeds and to examine the shock wave recovery downstream of the glow discharge. Radial shock profiles at several axial locations are experimentally determined by measuring the arrival time at different radial locations. These measurements are found to be in qualitative agreement with predictions from numerical simulations that consider temperature gradients and viscous effects, but which do not account for any effects of the plasma on shock propagation.

Nomenclature

V_s = shock propagation velocity
x = axial distance along the shock tube
ε = energy loaded into the shock tube gas by the spark discharge
μ = gas viscosity
ρ = gas density

I. Introduction

THE structure and propagation of shock waves in gases has been a topic of much interest in this century, motivated primarily by aerospace applications. It has been the subject of several authoritative books.[1–4] Shock propagation in plasmas has also been studied with specific regard to reentry flows, interaction of the solar wind with the terrestrial magnetosphere, and magnetohydrodynamic applications. This research has also culminated in several authoritative texts.[5–9] Despite this abundance of information on shock wave propagation in ionized and nonionized gases, experiments conducted in Russia[10–16] and in the United States[17–19] have prompted further inquiry on this problem.[20–23] Experiments reported in Refs. 17–19 show apparent modification of shock structure within a glow discharge and report lengths on the order of the shock tube diameter, to recover the original shock structure downstream of the discharge. Analysis of this problem by numerical solution of the inviscid Euler equations[20–23] has shown that radial temperature gradients created by the glow discharge could explain the experimental observations reported in Refs. 10–19.

In this paper, experimental results for the propagation of shock waves through weakly ionized argon are presented. The shock waves are generated using a capacitively discharged spark and subsequently launched into a low-pressure glow discharge in argon. The experimental apparatus is similar to that used in Refs. 17–19 and is described therein. In addition, measurements of the average shock velocity and shock structure are provided at several axial locations along the length of the tube, and at several radial locations for given axial positions. Shock structure is inferred by photoacoustic deflection (PAD) measurements.[17–19] Measurements recording the effects of reversing the direction of the electric field on shock propagation velocity and photoacoustic signal characteristics are also discussed. An important focus of this paper is examination of the recovery of the photoacoustic signal downstream of the glow discharge, as a function of distance along the tube.

This paper is organized as follows. The experimental apparatus and procedure are briefly described in the following section. Section III describes the experimental measurements and plausible explanations for these results. A summary is provided in Sec. IV, along with the conclusions of this work.

II. Experimental Apparatus and Procedure

The experimental apparatus consists of a 5-cm-diam closed Pyrex tube comprising a central glow discharge section. A Kolb tube[24] at one end houses the spark gap used to generate a shock wave. The spark gap consists of a pair of tungsten electrodes with a gap distance of 1 cm. The electrodes are cylindrical rods 0.3175 cm ($\frac{1}{8}$ in.) in diameter. The gas used in the measurements reported here is argon and is maintained at a pressure of 30 torr. Typically, a voltage of 10 kV is impressed across the spark gap, discharging approximately 25 J of energy over an approximate time interval of 1 μs. However, only a fraction of this energy from the capacitive discharge is loaded into the gas. A shock wave is subsequently formed as a result of the rapid energy addition and propagates through the tube. In the experiments involving a plasma, a glow discharge in 30 torr of argon is struck between the two electrodes located downstream of the spark gap. The electrodes in the glow discharge section are cylindrical, 2.5 cm in diameter, hollow, and concentric within the Pyrex shock tube, as can be seen in the schematic shown in Fig. 1. The argon gas is introduced via a rotameter and flows at 100 sccm (standard cubic centimeters per minute) in the direction counter to that of shock propagation as in Refs. 17–19. In Refs. 17–19, however, the flow was carefully controlled and introduced at a rate of 50 sccm using a mass flow controller. In an effort to reproduce one of the shock tube configurations of Refs. 17–19, the upstream electrode (i.e., nearest the spark gap) is longer, 5 cm in length, whereas the downstream electrode (i.e., farthest away from the spark gap) is shorter, 1.5 cm in length. The distance between the electrodes (edge to edge) in the glow discharge is 22.25 cm in the present work, and the corresponding distances in Refs. 17–19 were 19 and 20 cm. A visibly uniform glow discharge can be maintained in argon at 30 torr using this configuration, until the discharge current exceeds about 60 mA, after which point the discharge becomes filamentary. In the experiments reported here, the current in the glow discharge is varied from 0 to 50 mA, and the voltage is varied from 1.8 kV (for 10 mA) to 4.8 kV (for 50 mA). The discharge is operated for 15 min before shock waves are launched into the plasma, to ensure that any thermal gradients that exist would have attained steady state. This is especially important because the shock structure has been observed to be unchanged when the shock passes through immediately after the glow discharge is initiated.[25,26]

Received 17 November 2000; revision received 20 April 2001; accepted for publication 24 April 2001.

*Graduate Research Associate, Center for Advanced Plasma Engineering, Non-Equilibrium Thermodynamics Laboratories, Department of Mechanical Engineering.

†Professor, Center for Advanced Plasma Engineering, Non-Equilibrium Thermodynamics Laboratories, Department of Mechanical Engineering. Senior Member AIAA.

A Uniphase 1125 He–Ne laser (10 mW) is directed perpendicular to the axis of the shock tube, partially illuminating a Thor Laboratories PDA 155 high-speed amplified silicon detector on the other side of the tube, as shown in Fig. 1. The instant of spark initiation is relayed to the oscilloscope via a synchronization signal provided by the spark gap trigger. The oscilloscope is programmed with an appropriate delay after spark initiation to enable capture of the passing shock as it traverses the downstream location of the PAD detection system. The output of the detector is a voltage proportional to the intensity of the beam illuminating it. As the shock wave traverses across the laser beam, the gradient in density across the shock front gives rise to a variation in the index of refraction, causing the He–Ne beam to deflect. The resulting time-varying voltage is then recorded on a Tektronix digital oscilloscope (40 MHz). In the experiments reported here, a sampling rate of 5 MHz is used. The deflection of the beam is proportional to the axial density gradient integrated radially across the tube and results in a time-varying intensity recorded by the detector and which is output as a time-varying voltage. Therefore, a shock front would give rise to a PAD signal that appears as a sharp spike resembling a delta function. The same photoacoustic signal is used to measure the average velocity of the shock front. This is done by measuring the time of flight between two axial locations, 6.9 cm apart. In this instance, the He–Ne beam is passed through a beam splitter, one beam passing through the tube and illuminating a detector on the other side. The other beam is reflected off a mirror and then passed through the tube onto a second detector. Using the signal from the first detector as the trigger and prescribing a time delay then allows the shock wave arrival time to be determined at the second axial location. The travel time of the shock wave between the two locations is recorded, and because the distance between these locations is known, an average velocity can be calculated. The two split beams are separated by 6.9 cm due to physical limitations in the apparatus, which is coarser than the 2.59 cm separation used to measure the shock velocity in Refs. 17–19. The average shock velocity at a given point is, thus, measured by the time of flight between the split beams, 3.45 cm on either side of a point, in the present experiments. Variation of the average shock speed along the tube is determined by mounting the laser/detector assembly on an optical rail, which is then attached on a translation stage that traverses parallel to the shock tube. All measurements of the shock propagation speed within the glow discharge using the split beam were made with both beams within the glow region.

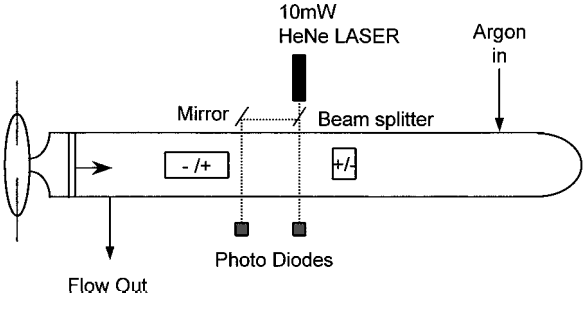

Fig. 1 Schematic of experimental apparatus.

In this paper, several experimental measurements are reported. Measurements of average shock speed are obtained at several axial locations. These are the regions before, within, and downstream of the glow discharge. These average velocity measurements are obtained for two discharge polarities, one where the applied electric field is in the same direction as shock propagation and the other in which the electric field is in the direction counter to that of shock propagation. Measurements of the average shock speed are also made for several values of the total current within the diffuse glow discharge: 0, 10, 30, and 50 mA. PAD signals are also obtained for these current levels and for both orientations of the applied electric field. In addition, shot-averaged shock arrival times are recorded for various radial locations at three axial positions to determine the shape of the shock front. These measurements are presented in the following section, along with an accompanying discussion of the results.

III. Experimental Results and Discussion

Shock propagation velocities along with the associated PAD signal characteristics are presented first. These results are obtained in the regions upstream of the glow discharge, within the glow discharge, and downstream of the glow discharge. The axial variation of the shock propagation speed is compared with theoretically expected trends for the viscous and inviscid cases. Recovery of the PAD signal after the shock exits the glow discharge is monitored. Finally, shot-averaged shock absolute arrival times are recorded radially for three axial locations upstream of and inside the glow discharge. These absolute arrival time measurements provide information regarding the shape of the shock front, to within shot-to-shot variation, and are compared with the numerical calculations presented in Ref. 27. These are compared with the PAD signal characteristics to infer the shape of the shock front.

Figure 2 shows a plot of the average shock propagation velocity as a function of position for the case where the longer (5-cm-long)

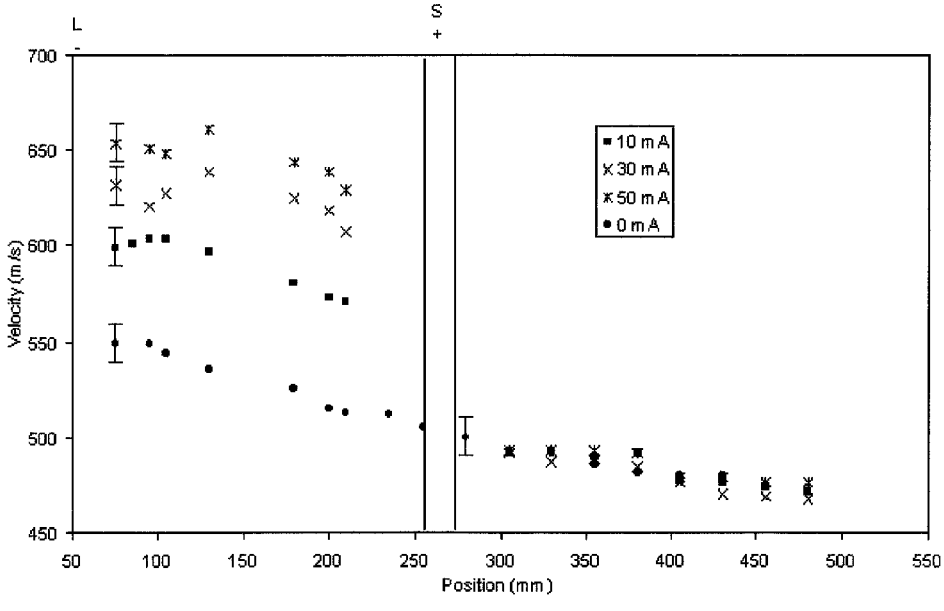

Fig. 2 Average shock propagation speeds measured vs distance along shock tube for various values of glow discharge current in *L*− glow discharge configuration.

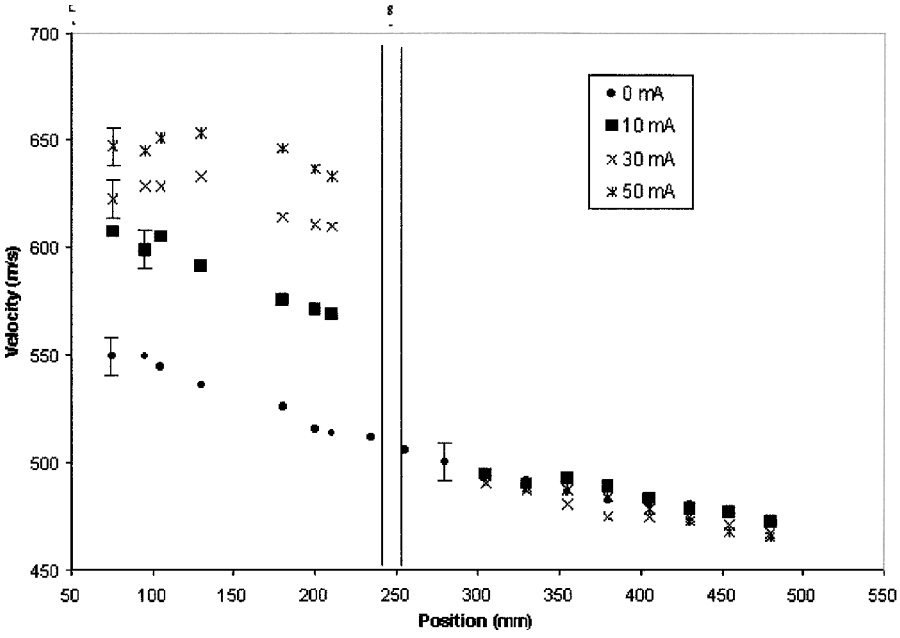

Fig. 3 Average shock propagation speeds measured vs distance along shock tube for various values of glow discharge current in *L*+ glow discharge configuration.

electrode located nearest to the spark gap is the cathode (denoted hereafter as $L-$) for different values of the total discharge current. In this case, the electric field is in the direction counter to that of shock propagation. Figure 3 shows the shock propagation speed vs axial position for the case where the longer electrode located nearest to the spark gap is the anode (denoted hereafter as $L+$) for different values of the total discharge current. Note from both Figs. 2 and 3 that, in the absence of the glow discharge, the shock propagation velocity decreases monotonically along the length of the shock tube. This is expected behavior and can be deduced from the following dimensional analysis.[3] The shock propagation speed in the inviscid case can be found by selecting the energy loaded into the gas by the spark discharge ε at the location $x = 0$, distance along the tube x, shock propagation velocity V_s, and density ρ as variables. If ε, x, and ρ are chosen as independent quantities, then the shock propagation speed can be expressed as

$$V_s \sim \sqrt{\varepsilon/\rho x^3} \tag{1}$$

Thus, in the case of inviscid expansion, the shock speed decreases monotonically as $x^{-3/2}$. For the viscous case, the set of variables includes ε, x, and V_s and is augmented by μ, the dynamic viscosity. If ε, x, and μ are chosen as the independent parameters, the shock speed is found to decrease as x^{-2}:

$$V_s \sim \varepsilon/\mu x^2 \tag{2}$$

The data in Figs. 2 and 3 in the absence of a glow discharge reveal a monotonic decrease in the shock propagation speed vs length along the tube. However, this decrease can be due to either the expansion itself or viscous effects. The experimental resolution is insufficient to distinguish between the $x^{-3/2}$ variation of Eq. (1) and the x^{-2} variation of Eq. (2). Hence, the effect of viscosity on shock propagation speed cannot be isolated from effects due to the expansion alone. This is important to bear in mind because viscous effects are expected to influence the PAD signal characteristics of weak shocks quite dramatically.[27,28] In contrast, for shocks of moderate strength considered here, the PAD signal characteristics in the absence of a discharge remain sharp and narrow all through the length of the tube.

Figures 2 and 3 also show shock propagation speeds vs length along the tube for various glow discharge currents, for the two orientations $L-$ and $L+$. In all cases, as mentioned in Sec. II, it was ensured that the rightmost of the two beams used to measure shock speed was within the glow discharge region. When the glow discharge is on, the shock speed exhibits a noticeable local maximum within the glow discharge section. Because the temperature within the glow discharge is uniform axially (see discussion later in this section), the shock speed should remain constant in the absence of viscous effects. However, the shock speeds in Figs. 2 and 3 exhibit a pronounced maximum in the middle of the glow region and, thus, cannot be explained by thermal effects alone. The maximum in the shock velocity, rather than a monotonic variation of the velocity in the glow discharge region, is due to the opposing influences of heating and wall shear. Ohmic heating within the discharge raises the gas temperature and, therefore, increases the shock velocity. On the other hand, wall shear becomes significant as the shock speed increases and ultimately serves to reduce the shock propagation speed. The effects of heating are evident in the observed increase in shock velocity as the current is raised. There is, however, a repeatable and noticeable local minimum in the shock velocity for the $L-$ case, near the cathode, for currents of 30 and 50 mA. More detailed experimental investigation suggests that the velocity dip is caused by the presence of the upstream electrode in the path of the shock wave.

On exiting the glow discharge section, the velocity of the shock can be seen to assume the same value as in the absence of the glow discharge, almost immediately. Figures 4 and 5 show PAD signals at several axial locations downstream of the glow discharge, for a representative discharge current of 10 mA and for the two orientations of electric field considered in this work. The same behavior is found for the higher currents (30 and 50 mA) as well. Evident in Figs. 4 and 5 is the recovery of the PAD signal to its delta-functionlike appearance on exiting the discharge. Typically, the PAD signal will increase in amplitude after the shock emerges from the glow discharge region, reach a maximum, and decline in amplitude thereafter. The recovery distance is defined here as the distance from the edge of the electrode at the end of the glow discharge to the axial location where the PAD signal recovers its delta-functionlike appearance. As can be seen from Figs. 4 and 5, there is a small but apparent dependence of the PAD signal recovery distance on the direction of the electric field. From Fig. 4, when the electric field is in the direction opposite to that of shock propagation, the recovery distance can be seen to be between 2.8 and 5.3 cm. In Fig. 5, when the electric field is aligned in the direction of shock propagation, the recovery distance is just beyond 5.3 cm, but very clearly before 7.8 cm. The recovery length is apparently longer when the electric field is in the direction of propagation of the shock, regardless of

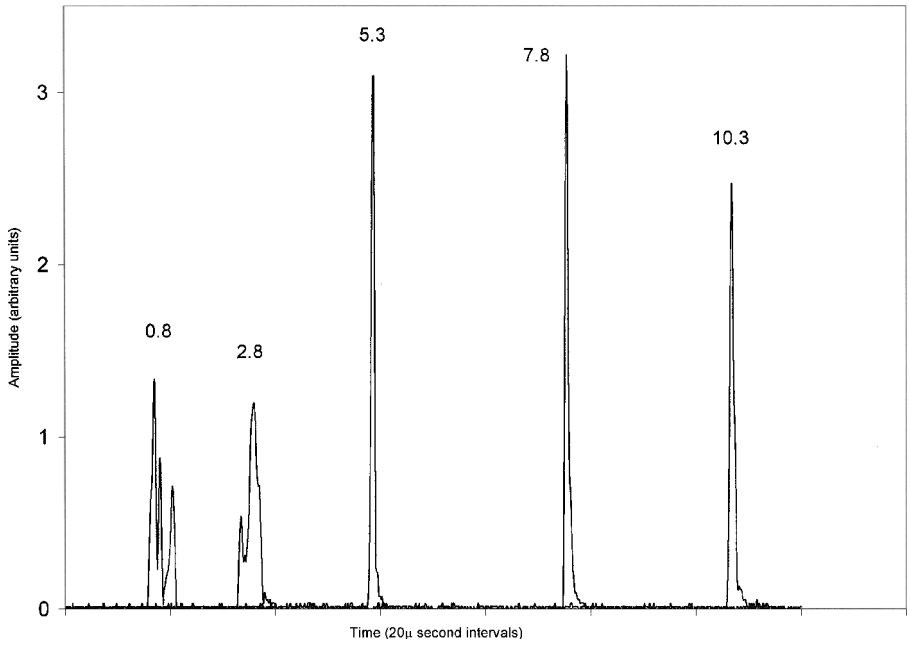

Fig. 4 Amplitude of PAD signal vs time, downstream of glow discharge, at various locations (indicated above PAD signals in centimeters ± 0.5 cm) from trailing edge of anode for *L*− configuration for discharge current of 10 mA.

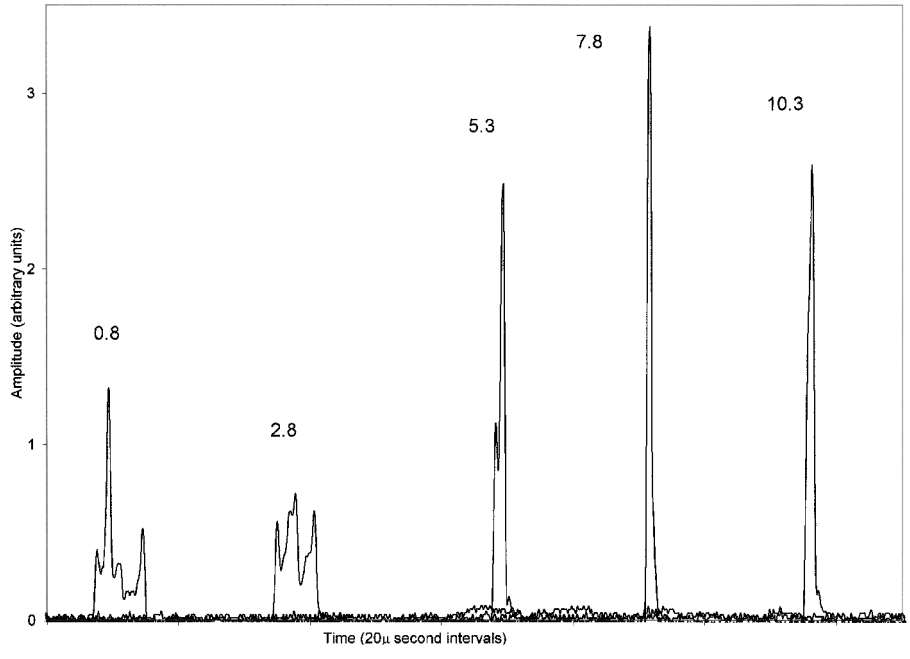

Fig. 5 Amplitude of PAD signal vs time, downstream of glow discharge, at various locations (indicated above PAD signals in centimeters ± 0.5 cm) from trailing edge of cathode for *L*+ configuration for discharge current of 10 mA.

the magnitude of the discharge current. In the instance where the electric field is oriented in the direction of shock propagation, the cathode, which is expected to be the hotter of the two electrodes, is on the downstream side of the shock propagation direction. Thus, the observed increase in recovery length for this case may have its origin in thermal effects associated with the electrode rather than the properties of the plasma. Note that variations up to 0.5 cm were observed due to shot-to-shot variation in the experiments reported here, making a determination of the exact recovery length impossible. The recovery distances of several tube diameters or more, observed in the present experiments, are consistent with results from the numerical simulations reported in Ref. 27. To determine the temperature of the glow discharge, CO was added to the argon as a thermometric element. Although addition of CO changes the discharge characteristics, the shock structure as determined by PAD signal measurements was found to be unaffected. The mixture comprised 3.3% CO and balance argon, but maintained the total pressure at 30 torr and the flow rate at 100 sccm. When CO is added to a discharge, C_2 is produced in an electronically excited state. When the resulting rotationally resolved Swan band emission from the C_2 molecules is measured, it is possible to determine the rotational temperature of the gas (see Ref. 29). The translational temperature is equivalent to the rotational temperature because these two modes are in equilibrium at these pressures. By the use of 0.5-cm-wide

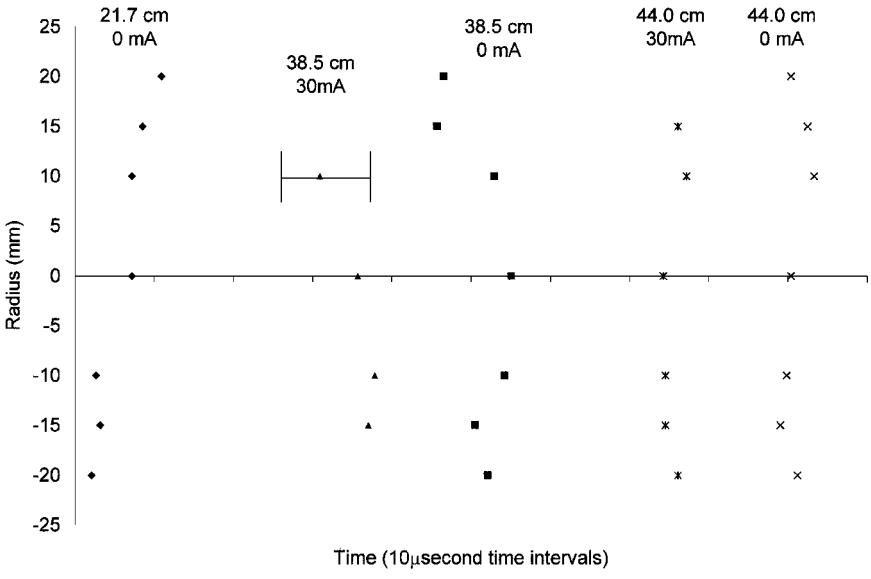

Fig. 6 Radial profile of passing shock front determined by measurement of absolute arrival time at axial locations upstream and within glow discharge; data for each axial location have been uniformly shifted by constant amounts [(21.7 cm, 0 mA) is shifted by −4 μs, (38.5 cm, 30 mA) is shifted by +14 μs, (38.5 cm, 0 mA) is shifted by +5 μs, (44 cm, 30 mA) is shifted by +35 μs, and (44 cm, 0 mA) is shifted by +20 μs to display radial profiles for different locations on the same figure].

apertures to view emission from a small region of the discharge, an average temperature distribution was inferred from the rotationally resolved Swan band spectra of C_2. This temperature represents an average value over the volume spanned by the cross section of the tube and the 0.5-cm width of the aperture. Measurements of the radial temperature distribution at several axial locations and of the axial temperature variation along the centerline were made for the $L-$ configuration. Only minute axial variation of the temperature (on the order of 10 K) was found. In the radial direction, temperatures were found to be 1009 K $\pm$ 200 K at the shock tube centerline, 1030 K $\pm$ 200 K at 2 cm above the centerline, and 909 K $\pm$ 200 K at 2 cm below the centerline. The temperatures determined using this method are within the same range as more detailed measurements undertaken by other groups.[25,26] The increase in shock propagation speed within the glow discharge region can, therefore, be attributed to the high temperatures associated with ohmic heating of the gas by the electrical discharge.

Thermal effects associated with the glow discharge plasma can explain acceleration of the shock as well as the splitting, spreading, and attenuation of the PAD signal. The high temperature within the glow discharge region serves to increase the local speed of sound and, thus, accelerates the shock wave. Moreover, because the pressure is constant, the density within the glow discharge region must be lower than that of the neutral gas outside the glow discharge. Therefore, the magnitude of the density gradient is also smaller within the glow discharge region, resulting in an attenuated PAD signal. In addition, there is a radial temperature gradient within the glow discharge region because the centerline has a high temperature ($\sim$1000 K) whereas the walls of the tube are relatively cool ($<$350 K). This causes the shock front to be curved near the wall, which in turn produces a split and spread PAD signal. Numerical simulations for both inviscid [20–23] and viscous cases [27] indicate that the shock does exhibit curvature in the presence of a radial thermal gradient and that this curvature causes splitting and spreading of the PAD signal comparable to that observed experimentally. Although this curvature is not pronounced (the near-wall regions of the shock front lag by $\sim$5 mm from the centerline segment of the front, as will be discussed next) it is, nevertheless, important enough to influence the highly sensitive PAD technique.

To quantify shock curvature experimentally, measurements were made of the absolute arrival times for several radial locations at a given axial position. Because only one laser source and detector were used in the present experiments, the data at different radial locations correspond to different shots, although they are for the same parameters governing the spark discharge used for shock generation. These results are shown in Fig. 6 before the shock enters the glow discharge and within the glow discharge region. Note that although absolute arrival times (i.e., measured from the instant the spark is initiated) are used to detect the shock front, the data for each axial location have been uniformly shifted by different amounts to display all of the results in Fig. 6. Note from Fig. 6 that to within shot-to-shot variation, the near-wall portions of the front differ in arrival time from the centerline portion by less than 7.7 μs. However, because the uncertainty due to shot-to-shot variation is greater than 10 μs, we may conclude that there is negligible curvature of the shock front. Given the measured shock speed of 625 m/s, the lag in arrival time of 7.7 μs corresponds to an axial distance of less than 5 mm. Note, therefore, that the shock front is largely planar, at least over the measured region spanning 4 cm of the 5 cm diameter. In the numerical results reported in Ref. 27, lag distances of about 9 mm can be inferred based on the staggered density profiles for the case of a shock significantly weaker in strength compared to the present experiments. Consequently, smaller lag distances are expected as the strength of the shock increases. Note, therefore, from both the present experiments and the numerical results of Ref. 27, that most of the shock front is planar, with curvature confined to the near-wall regions. The PAD signal is sensitive even to such small curvatures and, therefore, displays a split signal when the curvature is increased in the presence of radial temperature gradients or because of wall shear.[28]

In summary, most of the trends observed in the experiments reported here can be explained in terms of classical effects due to thermal gradients and wall shear. A plasma produces ohmic heating of the gas and generates radial thermal gradients. Shock acceleration can be easily explained by the higher temperatures present in the glow discharge. The experiments of Refs. 25 and 26 offer conclusive evidence for this. The splitting and spreading of the PAD signal does not imply splitting and spreading of the shock front itself. Rather, this observation can be explained by curvature of the shock front in the near-wall regions of the shock tube, which can be induced either by radial thermal gradients[20–23,27] or by the presence of wall shear alone.[27,28] Moreover, the recovery of the shock speed and the PAD signal downstream of the plasma is consistent with results from numerical simulations of shocks traversing through regions of thermal gradients alone, that is, in the absence of a plasma. Therefore, no plasma effects need to be invoked to explain the shock propagation characteristics observed in these or other experiments.[10–19,25,26]

IV. Conclusions

Shock propagation through a glow discharge has been examined using the PAD technique described in Ref. 17. The effects reported in Refs. 17–19 have been reproduced for argon at a pressure of 30 torr. The shock propagation speed has been measured vs distance along the direction of propagation and is influenced by gas heating and wall shear effects. Detailed measurements of the PAD signal recovery indicate a dependence on the direction of the electric field, which in turn appears to be caused by thermal effects stemming from the presence of a hot electrode (the cathode). Splitting and spreading of the PAD signal observed when the shock passes through the glow discharge can be explained by the presence of radial thermal gradients and wall shear. Radial thermal gradients and wall shear are capable of introducing curvature to the shock front, especially in the near-wall regions. However, measurements of shock arrival time at various radial positions within the glow discharge and away from the wall indicate no change in shock structure or shock planarity (to within shot-to-shot variation). Shock curvature does influence the PAD signal due to the sensitivity of this measurement and because the recorded PAD signal is line of sight averaged. This explains why the PAD signal appears split and spread as the shock passes through the glow discharge, whereas shock arrival time measurements indicate the shock front to be, for the most part, planar. In conclusion, the basic characteristics of shock propagation within a glow discharge appear to be explainable in terms of the classical effects of thermal gradients and wall friction, with no recourse to any plasma effects. Although an electrostatic space charge layer does indeed exist near the shock front and travels along with it, there is no evidence that this space charge layer actually alters the structure of the shock wave in the primarily neutral gas.

Acknowledgments

This work was supported by U.S. Air Force Office of Scientific Research Grant F49620-99-1-0023, monitored by Steven Walker. Support was also provided for major equipment in part by two Ohio Board of Regents Investment Fund Grants. The authors gratefully acknowledge many helpful discussions with B. Ganguly, P. Bletzinger, and A. Forlines of the U.S. Air Force Research Laboratory and W. Bailey of the Air Force Institute of Technology.

References

[1]Courant, R., and Friedrichs, K. O., *Supersonic Flow and Shock Waves*, Springer-Verlag, New York, 1976.

[2]Shapiro, A. H., *Dynamics and Thermodynamics of Compressible Fluid Flow*, Vols. 1 and 2, Ronald, New York, 1953.

[3]Zel'dovich, Ya. B., and Raizer, Yu. P., *Physics of Shock Waves and High-Temperature Hydrodynamic Phenomena*, edited by W. D. Hayes and R. F. Probstein, Vols. 1 and 2, Academic International Press, New York, 1966.

[4]Liepmann, H. W., and Roshko, A., *Elements of Gasdynamics*, Wiley, New York, 1957.

[5]Hughes, W. F., and Young, F. J., *Electromagnetodynamics of Fluids*, Wiley, New York, 1966.

[6]Tidman, D. A., and Krall, N. A., *Shock Waves in Collisionless Plasmas*, Wiley-Interscience, New York, 1971.

[7]Clauser, C. H., (ed.), *Plasma Dynamics*, Addison Wesley Longman, Reading, MA, 1960.

[8]Sutton, G. W., and Sherman, A., *Engineering Magnetohydrodynamics*, McGraw–Hill, New York, 1965.

[9]Pai, S. I., *Dynamics of Fluids and Plasmas*, Academic International Press, New York, 1966.

[10]Klimov, A. I., Koblov, A. N., Mishin, G. I., Serov, Yu. L., and Yavor, I. P., "Shock Wave Propagation in a Glow Discharge," *Soviet Technical Physics Letters*, Vol. 8, No. 4, 1982, pp. 192–194.

[11]Klimov, A. I., Koblov, A. N., Mishin, G. I., Serov, Yu. L., Khodataev, K. V., and Yavor, I. P., "Shock Wave Propagation in a Decaying Plasma," *Soviet Technical Physics Letters*, Vol. 8, No. 5, 1982, pp. 240–241.

[12]Evytyukhin, N. V., Margolin, A. D., and Shmelev, V. M., "On the Nature of Shock Wave Acceleration in Glow Discharge Plasma," *Soviet Journal of Chemical Physics*, Vol. 3, No. 9, 1986, p. 2080.

[13]Voinovich, P. A., Ershov, A. P., Ponomareva, S. E., and Shibkov, V. M., "Propagation of Weak Shock Waves in Plasma of Longitudinal Flow Discharge in Air," *High Temperature*, Vol. 29, No. 3, 1991, p. 468.

[14]Babaeva, N., "On the Structure of Shock and Blast Waves in Nonequilibrium Plasma of Gas Discharge," *Russian Journal of Chemical Physics*, Vol. 12, 1993, p. 357.

[15]Babaeva, N., Mnatsakanyan, A., and Naidis, G., "Modeling of Shock Wave Propagation in a Gas Discharge Developing in Nitrogen," *High Temperature*, Vol. 31, No. 4, 1993, p. 820.

[16]Babaeva, N., and Nadis, G., "Simulation of Shock Wave Propagation in Gas Discharge Plasma Regions," *Proceedings of the Workshop: Perspectives of MHD and Plasma Technologies in Aerospace Applications*, 1999, p. 108.

[17]Ganguly, B. N., Bletzinger, P., and Garscadden, A., "Shock Wave Damping and Dispersion in Nonequilibrium Low Pressure Argon Plasmas," *Physics Letters A*, Vol. 230, June 1997, pp. 218–222.

[18]Bletzinger, P., and Ganguly, B. N., "Local Acoustic Shock Velocity and Shock Structure Recovery Measurements in Glow Discharges," *Physics Letters A*, Vol. 258, July 1999, pp. 342–348.

[19]Garscadden, A., Bletzinger, P., and Ganguly, B. N., "Acoustic Shock Interaction in a Positive Column Plasma," AIAA Paper 99-4973, Nov. 1999.

[20]Bailey, W. F., and Hilbun, W. M., "Baseline of Thermal Effects on Shock Propagation in Glow Discharges," *Proceedings of the 1st Weakly Ionized Gases Workshop*, U.S. Air Force Academy, CO, June 1997, pp. GG3–GG18.

[21]Macheret, S. O., and Miles, R., "Shock Propagation in Weakly Ionized Plasmas: Mechanisms and Key Problems," *Proceedings of the 1st Weakly Ionized Gases Workshop*, U.S. Air Force Academy, CO, June 1997, pp. X-11–X-33.

[22]Macheret, S. O., Martinelli, L., and Miles, R. B., "Shock Wave Propagation and Structure in Nonuniform Gases and Plasmas," AIAA Paper 99-0598, Jan. 1999.

[23]Adamovich, I., Subramaniam, V. V., Rich, J. W., and Macheret, S. O., "Phenomenological Analysis of Shock Waves in Weakly Ionized Gases," *AIAA Journal*, Vol. 36, No. 5, 1998, pp. 816–823.

[24]Kolb, A. C., "Production of High Energy Plasmas by Magnetically Driven Shock Waves," *Physical Review*, Vol. 107, No. 2, 1957, pp. 345–350.

[25]Ionikh, Y. Z., Chernysheva, N. V., Meschanov, A. V., Yalin, A. P., and Miles, R. B., "Direct Evidence for Thermal Mechanism of Plasma Influence on Shock Wave Propagation," *Physics Letters A*, Vol. 259, Aug. 1999, pp. 387–392.

[26]Ionikh, Y. Z., Chernysheva, N. V., Yalin, A. P., Macheret, S. O., Martinelli, L., and Miles, R. B., "Shock Propagation Through Glow Discharge Plasmas: Evidence of Thermal Mechanism of Shock Dispersion," AIAA Paper 2000-0714, Jan. 2000.

[27]Aithal, S. M., and Subramaniam, V. V., "On the Characteristics of a Spark Generated Shock Wave," *Physics of Fluids*, Vol. 12, No. 4, 2000, pp. 924–934.

[28]White, A. R., and Subramaniam, V. V., "Effect of Wall Shear on the Propagation of a Weak Spark-Generated Shock Wave in Argon," *Physics of Fluids*, Vol. 13, No. 8, 2001, pp. 2441–2444.

[29]Flament, C., George, T., Meister, K. A., Tufts, J. C., Rich, J. W., Subramaniam, V. V., Martin, J. P., Piar, B., and Perrin, M. Y., "Nonequilibrium Vibrational Kinetics of Carbon Monoxide at High Translational Mode Temperatures," *Chemical Physics*, Vol. 163, No. 2, 1992, pp. 241–262.